(14) Cohen, A. S.; Terabe, S.; Smith, J. A.; Karger, B. L. *Anal. Chem.* **1987**, *59*, 1021-1027.
(15) Cohen, A. S.; Nagarian, D.; Smith, J.; Karger, B. L. *J. Chromatogr.* **1988**, *458*, 323-333.
(16) McCormick, R. M. *Anal. Chem.* **1988**, *60*, 2322-2328.
(17) Lauer, H. H.; McManigill, D. *Anal. Chem.* **1986**, *58*, 166-170.
(18) Walbroehl, Y.; Jorgenson, J. W. *J. Microcolumn Sep.* **1989**, *1*, 41-45.
(19) Jorgenson, J. W.; Lukacs, K. D. *Science* **1983**, *222*, 266-272.
(20) Hjerten, S. *J. Chromatogr.* **1985**, *347*, 191-198.
(21) Hjerten, S. *Chromatogr. Rev.* **1967**, *9*, 122-219.
(22) Herren, B. J.; Shafer, S. G.; Alstire, J. V.; Harris, J. M.; Snyder, R. S. *J. Colloid Interface Sci.* **1987**, *115*, 46-55.
(23) Towns, J. K.; Regnier, F. E. *J. Chromatogr.* **1990**, *516*, 69-78.
(24) Wiktorowicz, J. E.; Colburn, J. C. *Electrophoresis* **1990**, *9*, 769-773.
(25) Tsuda, T. *HRC & CC, J. High Resolut. Chromatogr. Chromatogr. Commun.* **1987**, *10*, 622-624.
(26) Huang, X.; Luckey, J. A.; Gordon, M. J.; Zare, R. N. *Anal. Chem.* **1989**, *61*, 766-770.
(27) Pfeffer, W. D.; Yeung, E. S. *Anal. Chem.* **1990**, *62*, 2178-2182.
(28) Desilets, C. R.; Rounds, M. A.; Regnier, F. E. *J. Chromatogr.*, in press.
(29) Borgerding, M. F.; Hinze, W. L. *Anal. Chem.* **1985**, *57*, 2183-2190.
(30) Landy, J. S.; Dorsey, J. G. *Anal. Chim. Acta.* **1985**, *178*, 179-188.
(31) Barford, R. A.; Sliwinski, B. J. *Anal. Chem.* **1984**, *56*, 1554-1556.
(32) Deschamps, J. R. *J. Liq. Chromatogr.* **1986**, *9* (8), 1635-1653.
(33) Chang, J. P. *J. Chromatogr.* **1984**, *317*, 157-163.
(34) Shihabe, Z. K.; Dyer, R. D. *J. Liq. Chromatogr.* **1987**, *10* (11), 2383-2391.
(35) DeLuccia, F. J.; Arunyanart, M.; Yarmchuk, P.; Weinberger, R.; Cline Love, L. J. *LC Magazine* **1985**, *3* (9), 794.
(36) Pertorius, V.; Hopkins, B. J.; Schieke, J. D. *J. Chromatogr.* **1974**, *264*, 385.
(37) Davies, J. T.; Rieal, E. K. *Interfacial Phenomena*; Academic Press: New York, 1961.
(38) Regnier, F. E. *Science* **1987**, *238*, 319.
(39) Novotny, M. *Anal. Chem.* **1988**, *60*, 500A-510A.
(40) Kalyanasundaran, K.; Thomas, J. K. In *Micellization, Solubilization, and Microemulsions*; Mittal, K. L., Ed.; Plenum Press: New York, 1977; Vol. 2, pp 569-588.
(41) Jorgenson, J. W.; Lukacs, K. D. *HRC & CC, J. High Resolut. Chromatogr. Chromatogr. Commun.* **1981**, *4*, 230-231.
(42) Huang, X.; Gordon, M. J.; Zare, R. N. *J. Chromatogr.* **1989**, *480*, 285-288.
(43) Lukacs, K. D.; Jorgenson, J. W. *HRC & CC, J. High Resolut. Chromatogr. Chromatogr. Commun.* **1985**, *8*, 407.

RECEIVED for review November 21, 1990. Accepted March 11, 1991.

Experimental Evaluation of Conflicting Models for Size Exclusion Chromatography

Syed Hussain,[1] Mamta S. Mehta,[1,2] Jerome I. Kaplan,[3] and Paul L. Dubin*[,1]

Departments of Chemistry and Physics, Indiana University-Purdue University, Indianapolis, Indiana 46205-2820

Comparisons were made among the predicted dependences of K_{SEC}, the chromatographic partition coefficient, on the solute radius R, for three widely acknowledged theories of size exclusion chromatography. It was found that data which appear to agree with the general form of $K(R)$ for any one theory will also appear to support the others, because of the mathematical relationships among the three $K(R)$ functions, over the range of K most usually reported. It must be concluded that the shape of the functional dependence of K_{SEC} on R alone does not provide a meaningful test of theory. To test these theoretical relations, data were obtained by aqueous SEC on Superose columns for molecular weight fractions of Ficoll. This solute may be shown to closely approximate a rather inflexible sphere, and hydrophobic and electrostatic interactions can be neglected for this polymer/stationary phase pair. The selection of conditions thus reduces uncertainties related to the definition of R and minimizes the influence of enthalpic effects (i.e., "nonideal SEC"). The measured dependence of K_{SEC} on R (with corrections made for polydispersity of the samples) is found to agree remarkably well with predictions from a treatment in which the stationary phase is modeled as a Gaussian distribution of cylindrical cavities.

INTRODUCTION

Size exclusion chromatography (SEC) is sometimes viewed as a liquid chromatographic separation technique, sometimes as a molecular weight method. It fulfills the latter role only when the column is calibrated with appropriate standards, and it is not always clear what constitutes an appropriate calibration. The requirement for calibration arises in part from the absence of a complete theory for SEC, which would exactly define the relationship between the macromolecular dimensions of the solute and the experimentally measurable chromatographic partition coefficient, K_{SEC}:

$$K_{SEC} = \frac{V_e - V_0}{V_t - V_0} \quad (1)$$

where V_e is the retention volume of the solute, V_0 the interstitial volume (obtained experimentally as the elution volume of a solute too big to enter the pores), and V_t the total volume of liquid in the column, equal to the sum of V_0 and the pore volume. K_{SEC} thus represents the fraction of the pore volume accessible to the solute and ranges from zero to unity. Despite decades of investigation, considerable debate still exists about the proper form of the theoretical relationship among K_{SEC}, pore size, and macromolecular dimensions. Therefore, conversion of SEC elution volumes to some well-defined dimension is not possible in the sense that say the measured diffusivity leads to an equivalent Stokes radius.

It is clear that the retention time in SEC—barring nonsteric interactions between the solute and the stationary phase—must depend uniquely on the dimensions of the solute and the stationary-phase pore. If these objects possessed simple geometry, the dependence of K on pore and solute sizes would take a very simple form; i.e.,

$$K = (1 - R/r_p)\lambda \quad (2)$$

where R is the radius of a spherical solute and r_p the pore radius and where $\lambda = 1$, 2, or 3 for slab, cylindrical, or spherical pores (*1*). (We designate K as the theoretical equilibrium constant equivalent to the relative solute concentration within the pore, C/C_0, and so distinguish it from the measured quantity K_{SEC}. It is important to note that K_{SEC} is equivalent to what others have called K_D, but different from K_{av}, which early workers defined as the fraction of the swollen gel ac-

[1] Department of Chemistry.
[2] Current address: Department of Chemistry, University of Illinois at Urbana-Champaign, Urbana, IL 61821.
[3] Department of Physics.

0003-2700/91/0363-1132$02.50/0

cessible to the solute.) The situation, however, is complicated by the ill-defined and possibly nonuniform geometries of both the cavities and the solute. Attempts to convert this problem to a tractable form have taken a variety of routes, in which, of necessity, the geometry of at least one of the two components is reduced to a simple form. Laurent and co-workers (2) used the treatment of Ogston (3) to model the separation as the diffusion of hard spheres of radius R through a concentrated solution of rigid rods. The result of this treatment may be expressed as

$$R = (-(\ln K_{av}/\pi l))^{1/2} - r_f \quad (3)$$

or

$$K_{av} = \exp[-\pi l(R + r_f)^2] \quad (3a)$$

where r_f is the rod radius (cross-sectional radius of the fibers that constitute the gel) and l is the linear concentration of rods in the gel (stationary phase). K_{av} is the probability that a spherical particle is included in the network of the gel and is related to K_{SEC} by the expression

$$K_{av} = K_{SEC}V_i/(V_i + V_m) \quad (4)$$

where V_i is the total pore volume and V_m is the volume of the gel matrix (the nonporous portion of the gel) in the column. (The sum $V_i + V_0 + V_m$ is the total geometric volume of the column; when this is referred to as "V_T", then K_{av} may unfortunately appear as $(V_e - V_0)(V_T - V_0)^{-1}$, with confusing similarity to eq 1.) Ackers (4) avoided any precise geometric description of the stationary phase, envisaging it as a collection of semiaccessible regions, each one having a probability of being permeated equal to unity for all solutes below some critical size, or zero, for all larger solutes. Assuming that this distribution of "pores" could be described via an error function, Ackers obtained

$$R = a_0 + b_0 \text{ erf}^{-1}(1 - K) \quad (5)$$

i.e.,

$$K = 1 - \text{erf}[(R - a_0)/b_0] \quad (5a)$$

In a gel with identifiable pore geometry, a_0 would be the average pore radius, which we designate henceforth as $\bar{r}_p$, and b_0 would be the standard deviation of the pore distribution, referred to later as Δr. Note that eq 5a is incorrect in the limit $R = 0$, since $(K)_{R\to 0} = 1 - \text{erf}(-a_0/b_0)$, whereas it should equal 1. (Equation 10b gives the corrected from of eq 5a, as shown later.)

In both of the preceding treatments, the solute is considered to be spherical. Such a description oversimplifies the shape of nearly all macromolecules of interest. Giddings took a more general view of solute dimensions and analyzed the permeation of capsule-shaped rigid solutes into a stationary phase modeled as a collection of randomly intersecting planes (5). This treatment leads to the result

$$K = \exp(-s\bar{X}) \quad (6)$$

where $\bar{X}$ is half of the mean projection length of the solute and s is the pore surface area per unit of free volume, i.e., a measure of the mean pore size.

For flexible chain macromolecules, one must recognize the statistical nature of solute dimensions, as represented by, for example, the mean square radius of gyration $\langle s^2 \rangle$. A theoretical treatment for flexible chains in cylindrical cavities of radius r_p leads to (6)

$$K = 4\sum_{m=1}^{\infty} \beta_m^{-2} \exp[-\beta_m^2(\langle s^2 \rangle / r_p^2)] \quad (7)$$

where β_m are the roots of the equation $J_0(\beta) = 0$, $J_0(\beta)$ denoting the Bessel function of the first kind of order zero. It may be shown that eq 7 predicts that a wide variety of chain macromolecules, eluted on a single column, should yield a common dependence of K_{SEC} on the product of the intrinsic viscosity and the molecular weight, $[\eta]M \sim R_\eta^3$, where R_η is frequently referred to as the hydrodynamic radius (7). The fact that this "universal calibration" (8) has been experimentally confirmed for numerous synthetic macromolecules has persuaded many polymer chemists to the position that R_η (less ambiguously referred to as the viscosity radius (9)) is the fundamental SEC parameter, much as empirical correlations of K_{SEC} with the Stokes radius have convinced many protein chemists that R_S is the controlling dimension.

All of the preceding expressions have some current support among experimentalists, yet we may hardly believe that all could be considered to be verified by experiment. We may cite uncertainties about the experimental values of r_p, λ, l, and s in the foregoing expressions as major difficulties in validation of these models. Nevertheless, the forms of the dependences of K on R predicted by these expressions would appear to be so different as to allow for elimination of incorrect models, given the high precision of experimental K_{SEC} attainable.

To some extent, it may be possible to attribute the current state of uncertainty to the ambiguity in the solute size R. In the case of proteins, all simple geometrical models are approximations, although hydrodynamic properties may be accounted for by ellipsoids with appropriate axes (10). (One must also recognize that the amphiprotic and partially hydrophobic nature of most globular proteins is likely to yield nonsteric interactions with many stationary phases and so disort the purely geometric behavior). For more highly asymmetric proteins, questions of orientation become more significant, lead to suggestions of "end-on insertion" (11). These problems of charge interactions and anisotropy are not encountered with synthetic, nonionic, hydrophilic macromolecules, but then one confronts the matter of size polydispersity, both in terms of variations in molecular weight and temporal fluctuations in dimensions for a given chain.

In order to resolve the foregoing difficulties, one would like to measure K_{SEC} for uniform well-characterized spheres. Attempts have been made to study the retention of latex particles in aqueous SEC, but these materials must be highly surface-charged to exhibit true solubility, and the suppression of the electrostatic component of the separation via salt addition appears to induce hydrophobic interactions with the packing (12). In the current work, we turn to Ficoll, a densely branched, hydrophilic, nonionic copolymer based on sucrose and epichlorhydrin (13). We attempt to demonstrate that this solute approximates a noninteracting sphere for the purposes of SEC analysis and to test some of the expressions noted above. In addition, we compare these results with ones obtained for pullulan, a nonionic, expanded flexible chain polysaccharide.

The present work consists of two parts. In the first section, we utilize data from the literature (14, 15) to see how well several of the equations noted above fit the results. Attempts to fit one set of data using various expressions are surprisingly rare in the literature. This process reveals the range of K_{SEC} values and the experimental precision needed to discern among the various models. In the second section, we treat data obtained by us for Ficoll fractions on a packed Suprose column and propose a model that fits the data quantitatively throughout a wide range of K_{SEC} values.

EXPERIMENTAL SECTION

Methods. Well-characterized, narrow molecular weight distribution (MWD) fractions of pullulan were obtained from Shodex Corporation (Tokyo, Japan). Fractions of Ficoll, prepared by fractionation on Sepharose 4B or G-200 superfine and characterized by SEC and light scattering, were kindly provided by Dr. K. Granath of Pharmacia AB (Uppsala, Sweden). Characteristics of these fractions are described in Table I.

Table I. Description of Ficoll and Pullulan Samples

sample name	MW	$\bar{M}_w/\bar{M}_n$
Ficoll T 1800, fr. 9	714 000[a]	1.91[b]
Ficoll T 1800, fr. 12	461 000[a]	1.80[b]
Ficoll T 1800, fr. 15	321 000[a]	1.36[b]
Ficoll T 1800, fr. 20	132 000[a]	1.18[b]
Ficoll T 2850IVB, fr. 3	62 500[c]	1.13[b]
Ficoll T 2850IVB, fr. 11	21 800[c]	1.07[b]
pullulan P-800	811 000[d]	1.14[f]
pullulan P-400	384 000[d]	1.12[f]
pullulan P-200	188 000[d]	1.13[f]
pullulan P-100	107 000[d]	1.10[f]
pullulan P-50	48 000[e]	1.09[f]
pullulan P-20	20 800[e]	1.07[f]
pullulan P-10	12 200[e]	1.06[f]
pullulan P-5	5 300[e]	1.07[f]

[a] $\bar{M}_w$, from light scattering, by supplier. [b] From size exclusion chromatography, by supplier. [c] From size exclusion chromatography and light scattering, extrapolated from other fractions, by supplier. [d] Values reported from light scattering by Kato et al. (*16*). In some cases, these differ slightly from those given by the supplier. [e] Values reported from sedimentation equilibrium by Kawahara et al. (*17*). In some cases, these differ slightly from those given by the supplier. [f] As reported by supplier.

Intrinsic viscosities were measured by using a Schott AVN automatic viscometer at 25 °C. Diffusion coefficients were obtained by dynamic light scattering with a Model 801 Oros instrument (Cambridge, MA) on 2–5 g/L polymer solutions, except for the lowest molecular weight pullulan samples, i.e., 10 g/L for P-10 and 20 g/L for P-5. (This instrument incorporates a solid-state 35-mW laser to irradiate the sample in a 7-μL cell; 90° scattering is detected with an avalanche photodiode, and the resultant autocorrelation curve is analyzed by the method of cumulants to yield the *z*-average diffusion coefficient.)

All chromatography was carried out on a Superose 12 column, kindly provided by Dr. L. Hagel of Pharmacia AB. A Milton Roy minipump delivered eluant at a flow rate of about 0.5 mL/min (with 0.1% precision). Sample was injected with a Rheodyne 7010 injector and detected with a Waters R401 differential refractometer. All elution volumes were measured in triplicate, with reproducibility of better than ±0.05 mL. Elution volumes were converted to K_{SEC} via eq 1. V_0 was obtained from the elution of DNA as 8.05 mL, a value also consistent with the extrapolation of data for pullulan fractions to MW > 10^6. V_t was obtained as the elution volume for acetone or D_2O, 21.80 mL, thus giving a pore volume of 13.75 ± 0.08 mL. The consequent reliability of K_{SEC} may be estimated as ±1%.

All chromatography, viscometry, and dynamic light scattering were done in 0.38 M sodium nitrate–sodium phosphate buffer (9:1) at pH 5.5 (this buffer has been found to minimize the electrostatic effect of dissociated groups on Superose without appreciably enhancing hydrophobic interactions) (*18*).

Calculations. Evaluation of eq 11b was accomplished by using the software program "Mathematica" on a Macintosh II computer.

RESULTS AND DISCUSSION

Data obtained by Haller et al. for dextrans on porous glass packings (*14*) were plotted as R_S vs $1 - K_{SEC}^{1/2}$, R_S vs $(-\ln K_{av})^{1/2}$, and R_S vs $\text{erf}^{-1}(1 - K_{SEC})$, in order to test the expression put forward by Waldmann-Meyer (*1b*) (referred to by that author as "GEM" for "geometric exclusion model"), the expression of Laurent and Killander (*2c*), and the relationship developed by Ackers (*4*), respectively. Stokes radii were calculated from MWs by using an empirical relationship between the diffusion coefficient and MW obtained by Amu (*19, 20*):

$$D_0 = 1.1 \times 10^{-4} \bar{M}_w^{-0.51} \quad (8)$$

where the units of D_0 are, as usual, $cm^2\ s^{-1}$, along with

$$R_S\ (Å) = kT/(6\pi\eta D_0)10^{22} \quad (9)$$

where η is the viscosity of water at 20 °C, i.e., 0.0010 P. The

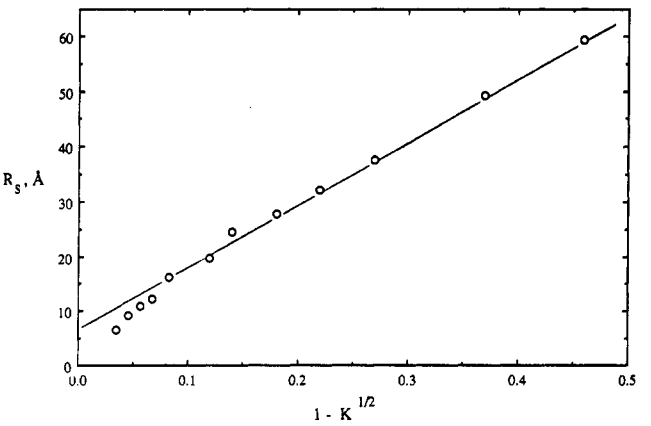

Figure 1. R_S vs $1 - K_{SEC}^{1/2}$, data from ref 14.

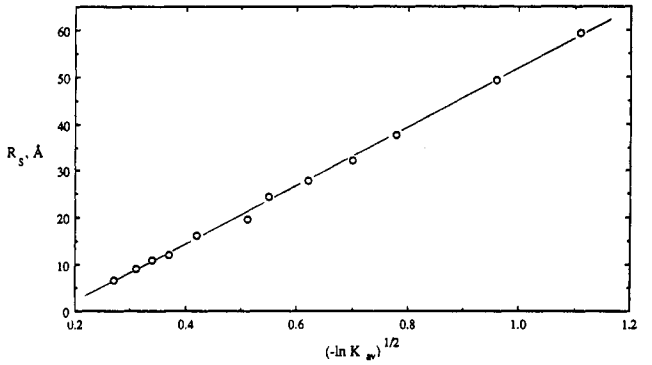

Figure 2. R_S vs $(-\ln K_{av})^{12}$, data from ref 14.

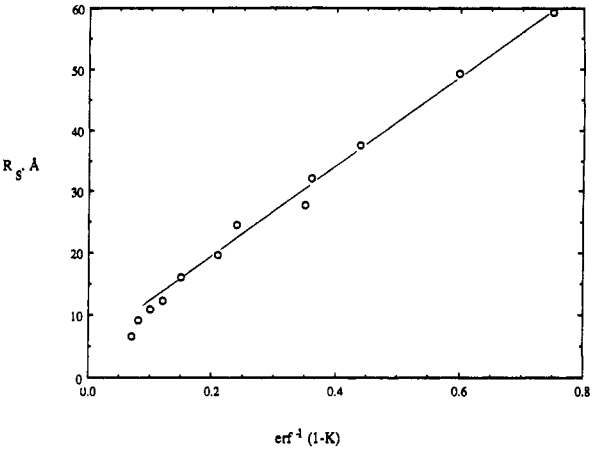

Figure 3. R_S vs $\text{erf}^{-1}(1 - K_{SEC})$, data from ref 14.

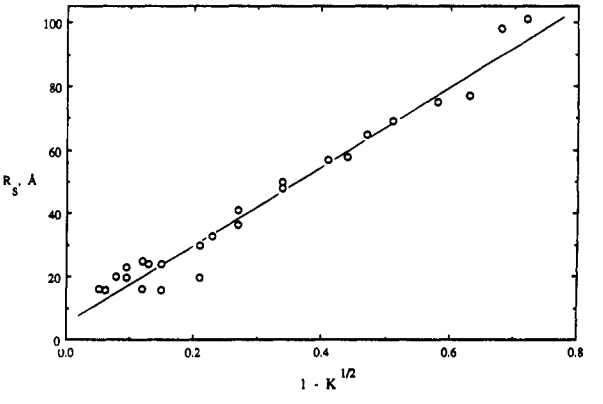

Figure 4. R_S vs $1 - K_{SEC}^{1/2}$, data from ref 15.

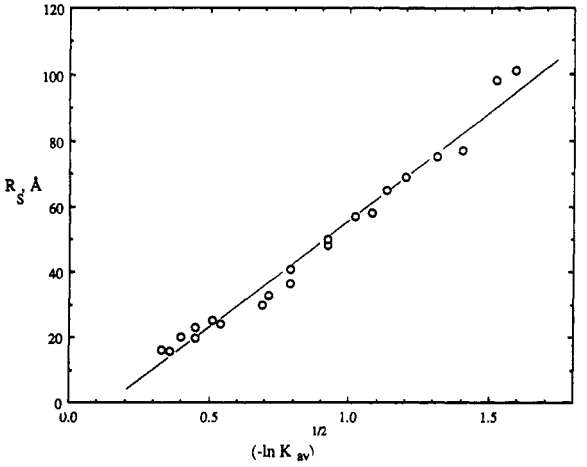

Figure 5. R_S vs $(-\ln K_{av})^{1/2}$, data from ref 15.

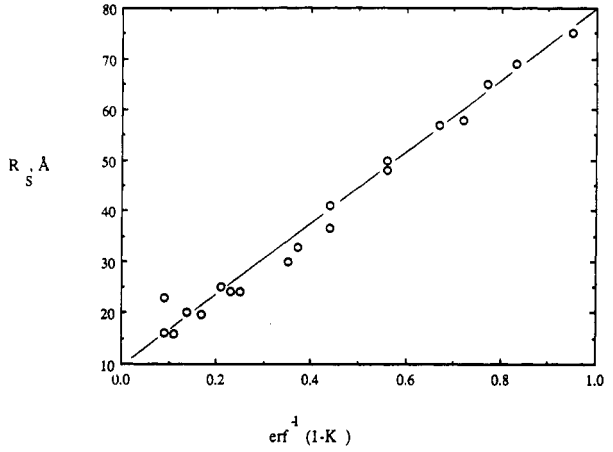

Figure 6. R_S vs $\text{erf}^{-1}(1 - K_{SEC})$, data from ref 15.

resultant plots are shown in Figures 1–3. Similar analyses were done with the data for dextrans on Sephadex G-200 obtained by Poitevin and Wahl, as shown in Figures 4–6. Nearly all the fits are seen to be very good, with regression coefficients for the GEM, Laurent–Killander, and Ackers plots of 0.991, 0.990, and 0.990, respectively, for dextran on G-200. Regression coefficients at least this good are seen for the dextran/porous glass data, with the sole exception of the GEM plot, which shows a discontinuity at $K = 0.77$.

The simultaneous agreement of the data with such different expressions is to some extent a purely mathematical effect. This may be seen in Figures 7–9, in which we plot $\text{erf}^{-1}(1 - K_{SEC})$ vs $1 - K_{SEC}^{1/2}$; $\text{erf}^{-1}(1 - K_{SEC})$ vs $(-\ln K_{av})^{1/2}$; and $(-\ln K_{av})^{1/2}$ vs $1 - K_{SEC}^{1/2}$, respectively. It is evident that agreement of the data with the functional form of the expression is not an adequate way to distinguish among the GEM, Laurent–Killander, and Ackers models, particularly if the data are confined to the region $0.05 < K_{SEC} < 0.7$. It is possible to discern between the Ackers and Laurent–Killander predictions for $K > 0.6$, but in order to distinguish between the goodness of fits to data for the GEM vs Laurent–Killander plots, one must have data at $K_{SEC} > 0.9$. It is virtually impossible to discern between the predictions of GEM and Ackers, since deviations from linearity are only observed at $K_{SEC} < 0.07$, i.e., near the exclusion limit.

The foregoing makes it clear that agreement of data with the functional form of an expression alone is an inadequate test of theory; one must compare the absolute values of K_{SEC} predicted and measured. In this regard, we note that, despite the good correlations of Figures 3 and 6, the Ackers treatment leads to an unrealistic result: the intercepts, which should

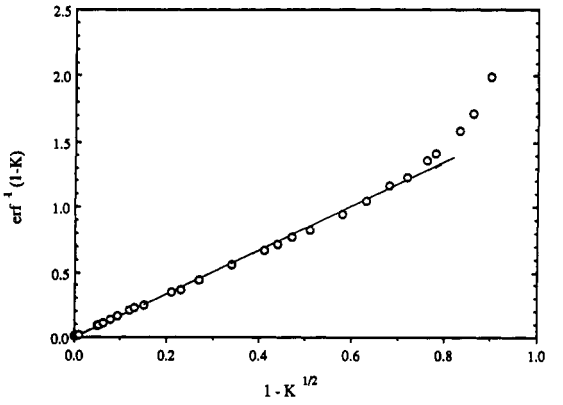

Figure 7. $\text{erf}^{-1}(1 - K_{SEC})$ vs $1 - K_{SEC}^{1/2}$. Arbitrary values chosen for K_{SEC}. Linear regime shows that the goodness of fit for the dependence of R_S on K_{SEC} for $K_{SEC} \geq 0.15$ could not distinguish between the Ackers and GEM models.

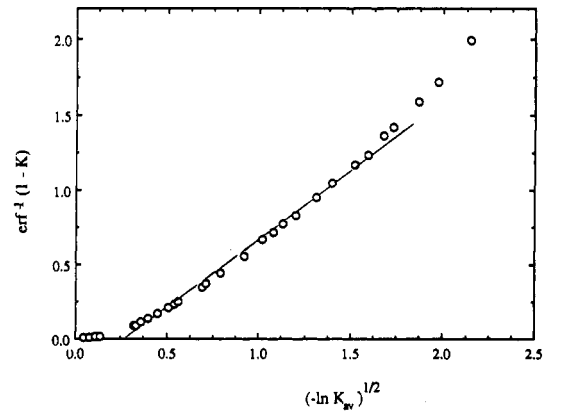

Figure 8. $\text{erf}^{-1}(1 - K_{SEC})$ vs $(-\ln K_{av})^{1/2}$. Arbitrary values chosen for K_{SEC}. Linear regime shows that the goodness of fit for the dependence of R_S on K_{SEC} for $0.02 < K_{SEC} < 0.61$ could not distinguish between the Ackers and Laurent–Killander models.

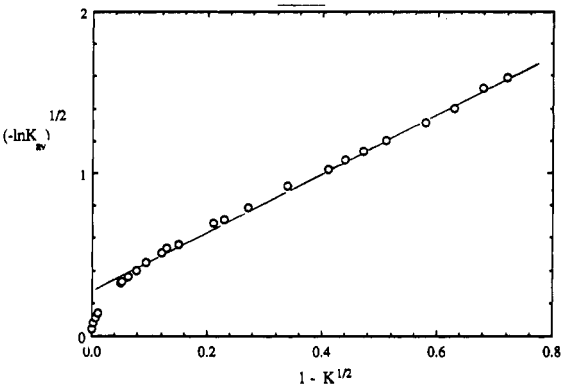

Figure 9. $(-\ln K_{av})^{1/2}$ vs $1 - K_{SEC}^{1/2}$. Arbitrary values chosen for K_{SEC}. Linear regime shows that the goodness of fit for the dependence of R_S on K_{SEC} for $K_{SEC} < 0.80$ could not distinguish between the GEM and Laurent–Killander models.

correspond to the mean pore radius, are about 10 Å for both Sephadex G-200 and porous glass.

The Ackers treatment contains the incorrect assumption that a monodisperse spherical solute will be either totally excluded by or else have full access to any pore. In this model, the dependence of K on R arises uniquely from the pore size distribution (PSD) and would, in fact, disappear for an infinitely narrow PSD. The fact that calibration curves (K vs R) do not become infinitely steep when the PSD narrows confirms the need for partial permeation, as found in the GEM model. On the other hand, the GEM model as formerly

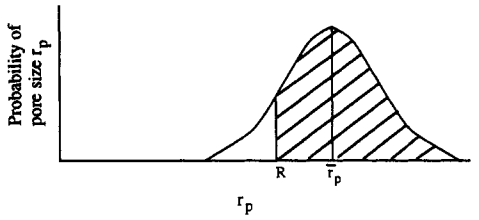

Figure 10. Depiction of the Ackers model. Shaded area represents fraction of pore volume accessible to a solute of radius R.

proposed (*1b*) does not take into account the effects of the finite PSD expected in most SEC columns. Thus, some combination of these two treatments would seem to have merit.

Incorporation of the pore size distribution into a geometrically simple model comprising cylindrical pores begins with the approach put forward by Ackers (*4*), which follows from Figure 10. As illustrated, Ackers assumed that $K = 1$ for solutes with radius R less than r_p and $K = 0$ for solutes with $R > r_p$. Consequently, one may write

$$K = \frac{\int_R^\infty e^{-(r_p-\bar{r}_p)^2/\Delta r^2}\, dr_p}{\int_0^\infty e^{-(r_p-\bar{r}_p)/\Delta r^2}\, dr_p} \tag{10a}$$

or

$$K = \frac{\text{erfc}\left[\dfrac{R-\bar{r}_p}{\Delta r}\right]}{\text{efc}\left[\dfrac{-\bar{r}_p}{\Delta r}\right]} \tag{10b}$$

where Δr is the width of the distribution of pore sizes, $\bar{r}_p$ is the mean pore radius, and erfc may be found in mathematical tables (*21*). Note that erfc $x = 1 - \text{erf}\, x$. One notes from eq 10b that $K = 1$ when $R \to 0$ and $K \to 0$ when $R \gg \bar{r}_p$, as required. However, as noted above, this treatment incorrectly predicts that size separation would not occur on a substrate with infinitely narrow pore size distribution. To include the geometric weighting as given in eq 2, one simply modifies eq 10a as

$$K = \frac{\int_R^\infty (1 - R/r_p)^\lambda e^{-(r_p-\bar{r}_p)^2/\Delta r^2}\, dr_p}{\int_0^\infty e^{-(r_p-\bar{r}_p)^2/\Delta r^2}\, dr_p} \tag{11a}$$

or

$$K = \frac{\int_{(R-\bar{r}_p)/\Delta r}^\infty \left(1 - \dfrac{R}{x\Delta r + \bar{r}_p}\right)^\lambda e^{-x^2}\, dx}{\dfrac{\sqrt{\pi}}{2}\,\text{erfc}\,(-\bar{r}_p/\Delta r)} \tag{11b}$$

from which K can be obtained by numerical evaluation. The exact choice of λ is problematic; given the irregular pore structure of gels such as Superose, there is no reason to expect any single, well-defined geometry. We have attempted to empirically determine the correct value of λ on Superose 12 by fitting data for various polymers to plots of R vs $1 - K^{1/\lambda}$. The goodness of fit has been found to be rather insensitive to λ, in the range $2 < \lambda < 3$. In what follows, we have employed $\lambda = 2$, which is supported by results obtained here (*22*) and elsewhere (*1b*).

An adequate test of the preceding information requires a knowledge of R for the samples chosen. The ambiguity that arises from either asymmetric compact macromolecules (e.g., proteins) or symmetric but highly flexible and solvated macromolecules (e.g., dextrans) could be resolved with a compact symmetric macromolecule. The compactness of Ficoll is less than that of proteins in that the intrinsic viscosity varies as approximately the cube root of the molecular weight (*23, 24*) (i.e., the Mark–Houwink exponent, $a \simeq 0.3$). This value for a is intermediate between the result for proteins ($a \simeq 0.1$) and dextran ($a \simeq 0.7$). However, Ficoll may still be considered to exhibit the hydrodynamic properties of a sphere, on the basis of the excellent agreement between its hindered diffusion through porous membranes with the theoretical predictions for a solid sphere (*25*), as well as differences observed between its diffusion in concentrated protein solutions and that of dextran (*26*).

Table II. Measured Characteristics of Ficoll Fractions

fraction	D, cm^2 s^{-1} × 10^8	$[\eta]$, dL g^{-1}	V_e, mL[a]	K_{SEC}[b]
T 1800, fr. 9	1.37	0.21, 0.19[c]	8.56	0.037
T 1800, fr. 12	1.77	0.17[c]	8.59	0.039
T 1800, fr. 15	2.10	0.15, 0.15[5c]	9.93	0.137
T 1800, fr. 20	3.52	0.121[c]	11.69	0.264
T 2850IVB, fr. 3	4.89	0.100[c]	12.93	0.354
T 2850IVB, fr. 11	8.16	0.074[c]	14.93	0.500

[a] Peak elution volume on Superose 12. [b] From values in the preceding column. [c] Based on reported $\bar{M}_w$ and $[\eta] = 0.005\bar{M}_w^{0.27}$ (*23*).

In obtaining the required K_{SEC} vs R plots for Ficoll, we confront the problem of polydispersity, which is as large as 1.9 for the highest MW sample (see Table I). While dimensions may be calculated from either the intrinsic viscosity $[\eta]$ or the diffusion coefficient D_0, these two variables correspond to two different moments of the distribution (the viscosity-average and z-average respectively), while the chromatographic peak (from which we obtain K_{SEC}) corresponds to yet a third. We chose to normalize all our data to the z-average component, by the following procedure, similar to one previously published (*27*). First an iterative procedure was used to obtain the correct Ficoll calibration curve, the criterion being that this plot of log M vs V_e must lead, in conjunction with the Ficoll chromatograms, to the $\bar{M}_w$ values from light scattering. The smooth curve so obtained yielded $\bar{M}_w$'s within 25% of the absolute values. This calibration curve could therefore be used to transform the chromatograms to the absolute MWDs, from which we computed the ratios $\bar{M}_z/\bar{M}_w$ and $\bar{M}_w/\bar{M}_v$, using, for the latter, the value of the Mark–Houwink exponent $a = 0.27$ (*23*). The absolute value of $\bar{M}_z$ for each fraction was obtained by multiplying the absolute value of $\bar{M}_w$ by the former ratio. We could then calculate the z-average intrinsic viscosity as

$$[\eta]_z = 0.50\bar{M}_z^{0.27} \tag{12}$$

from the viscosity–MW relationship of Granath (*23*). Then, the viscosity radius corresponding to the component of the distribution with the z-average MW is (*7*)

$$(R\eta)_z = \{3[\eta]_z\bar{M}_z/4\pi(0.025)N_A\}^{1/3} \tag{13}$$

$(R\eta)_z$ is obtained in cm when the units of $[\eta]$ are dL/g. As shown in Table II, measured values for $[\eta]$ agreed with the ones calculated according to eq 12. From the chromatograms, we could identify the elution volume corresponding to $\bar{M}_z$, i.e. $(V_e)_z$, from which we calculated $(K_{SEC})_z$. The last variable of interest, the Stokes radius, needs no such manipulations, since the quantity determined by dynamic light scattering is $R_S = (R_S)_z$ (*28*). The results of the foregoing calculations are summarized in Table III. It is important to note that, for the three lower MW Ficolls, the values of the Stokes radius and

Table III. Calculated Quantities for Ficoll Fractions

fraction	$\bar{M}_w$ (SEC)[a]	$\bar{M}_{z,calc}$[b]	$\bar{M}_v$ (SEC)[c]	R_S[d]	$(R_\eta)_z$[e]	$(V_e)_z$[f]	K_z[g]
T 1800, fr. 9	720000	830000	540000	160	138	8.40	0.0147
T 1800, fr. 12	510000	530000	478000	134	113	8.76	0.0411
T 1800, fr. 15	410000	353000	337000	113	95.5	9.66	0.107
T 1800, fr. 20	148000	156000	140000	67.4	67.7	11.18	0.219
T 2850IVB, fr. 3	77000	77000	73500	48.5	50.2	12.18	0.292
T 2850IVB, fr. 11	23400	23000	23000	28.8	30.0	14.52	0.464

[a] Computed from chromatogram and primary calibration curve (see text). [b] Computed as $\bar{M}_w$ (SEC)$(\bar{M}_z/\bar{M}_w)$, where the second term is obtained from the chromatogram along with the primary calibration curve. [c] Computed from chromatogram and primary calibration curve, with a = 0.27. [d] Stokes radius (Å); from column 1 of Table II. [e] z-Average viscosity radius (Å); from column 2, as $(R_\eta)_z$ (cm) = $[(0.50\bar{M}_z^{1.27})0.3/\pi N_A]^{1/3}$. [f] Elution volume for the component with the z-average MW (mL); obtained from primary calibration curve along with $\bar{M}_z$ from column 2. [g] z-Average chromatographic partition coefficient, from column 6.

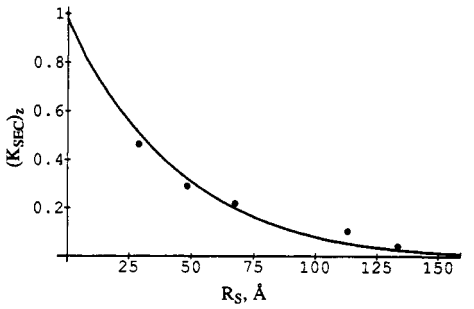

Figure 11. Comparison of experimental and theoretical dependence of K on R. Solid line: results from eq 11b, with $\bar{r}_p$ = 120 Å and Δr = 70%. Points are experimental results for Ficoll, with $(K_{SEC})_z$ calculated as described in the text and in Table III, and R_S calculated from the diffusion coefficient obtained by QELS.

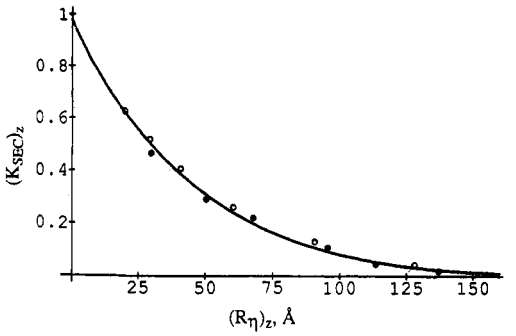

Figure 12. Comparison of experimental and theoretical dependence on K on R. Same as for Figure 11, but with $(R_\eta)_z$, calculated as described in the text and in Table III. Open circles are experimental results for pullulan, as R_η vs K_{SEC} (no adjustments for polydispersity required).

viscosity radius agree to within 3% (i.e., within experimental error), which confirms the correctness of viewing them as very compact spheres. (For pullulan, the viscosity radius becomes significantly larger than the Stokes radius when molecular weight exceeds 20000.) The ca. 17% discrepancy at larger MW could arise from more expanded dimensions for the larger solutes, although we note that if the value of a = 0.35 reported by Ficoll by Lavrenko et al. (*24*) were used instead of 0.27, this difference would be diminished (*29*).

In order to construct theoretical plots of K vs R according to eq 11b, values for the mean pore radius and its distribution were required. Two procedures to estimate $\bar{r}_p$ were employed, one identifying the slope of the measured R_S vs $1 - K_{SEC}^{1/2}$ with $1/\bar{r}_p$ (*1b*) and the other identifying $\bar{r}_p$ with R_S for the largest excluded fraction of pullulan. Both yielded a value of ca. 120 Å for $\bar{r}_p$. Some indication of the pore size distribution of Superose is provided by Hagel (*30*); we used several values in the expected range 40, 60, and 70% standard deviations. However, theoretical and experimental curves invariably crossed in the vicinity of K = 0.2, as shown for example in Figure 11. The best agreement was found upon comparison of theoretical K vs R curves with experimental K_z vs $(R\eta)_z$, as shown in Figure 12. The data conform to the predicted curve within experimental error over the entire experimentally accessible range. This last observation is consistent with other reports to the effect that a flexible chain macromolecule has the same SEC migration velocity as a sphere of equal viscosity radius, which were based on comparisons of the chromatographic partition coefficient for dextran vs proteins (*31*), pullulan vs proteins (*32*), moderately high MW DNA vs proteins (*9*), or pullulan vs surfactant micelles (*33*). On the other hand, the differences between the viscosity radii and the Stokes radii for pullulan are not so large as to establish that K vs R_S plots for the two types of polymers truly diverge. The question of the SEC dimension for asymmetric and expanded flexible chain polymers will be discussed in a separate report.

CONCLUSIONS

The apparent agreement between experimental data and the predictions of several widely divergent models for SEC is based, in part, on the mathematical nature of the proposed functions and the experimental difficulty of testing the proposed expressions in a quantitative manner, over a wide range of K. A simplified treatment for SEC of spherical solutes, based on modeling the stationary phase as a Gaussian distribution of cylindrical pores, reproduces the experimental K_{SEC} vs R_η plots for both the compact cross-linked polysaccharide, Ficoll, and the expanded linear polysaccharide, pullulan. The required parameters for mean pore size and pore size distribution are in good agreement with independent measurements of these variables. Further experiments, which must similarly be carried out under conditions in which solute-packing interactions are negligible, will be required to convincingly demonstrate the validity of this approach to other macromolecules.

ACKNOWLEDGMENT

The kind assistance of the following individuals is gratefully acknowledged. Lars Hagel, of Pharmacia AB, for the gift of Superose columns; K. Granath, also of Pharmacia, for kindly providing characterized molecular weight fractions of Ficoll; F. Lanni, of Carnegie-Mellon University, and K. Luby-Phelps of the University of Texas—Austin, for helpful advice about Ficoll.

LITERATURE CITED

(1) Casassa, E. F.; Tagami, Y. *Macromolecules* **1969**, *2*, 14. (b) Waldmann-Meyer, H. *J. Chromatogr.* **1985**, *350*, 1.
(2) Laurent, T. C.; Bjork, I.; Pietruszkiewitz, A.; Persson, H. *Biochim. Biophys. Acta* **1963**, *83*, 351. (b) Laurent, T. C.; Persson, H. *Biochim. Biophys. Acta* **1964**, *83*, 351. (c) Laurent, T. C.; Killander, J. *J. Chromatogr.* **1964**, *14*, 317.
(3) Ogston, A. G. *Trans. Faraday Soc.* **1958**, *54*, 1754.
(4) Ackers, G. K. *Adv. Prot. Chem.* **1970**, *24*, 343.
(5) Giddings, J. C.; Kucera, E.; Russell, C. P.; Meyers, M. N. *J. Phys. Chem.* **1968**, *78*, 397.

(6) (a) Casassa, E. F. J. Phys. Chem. 1971, 75, 275. (b) Casassa, E. F. J. Polym. Sci., Part B 1967, 5, 773.
(7) Flory, P. J. Principles of Polymer Chemistry; Cornell University Press: Ithaca, NY, 1953; p 606.
(8) Grubisic, Z.; Rempp, R.; Benoit, H. J. Polym. Sci.: Part B 1967, 5, 753.
(9) Potschka, M. Anal. Biochem. 1987, 162, 47.
(10) Cantor, P. R.; Schimmel, P. R. Biophysical Chemistry, Part II. Techniques for the Study of Biological Structure and Function; W. H. Freeman: New York, 1980; p 560.
(11) (a) Nozaki, Y.; Schechter, N. M.; Reynolds, J. A.; Tanford, C. Biochemistry 1976, 15, 3884. (b) Meredith, S. C.; Nathans, G. R. Anal. Biochem. 1982, 121, 234.
(12) Styring, M. G.; Davison, C. J.; Price, C.; Booth, C. J. J. Chem. Soc., Faraday Trans. 1, 1984, 80, 3051.
(13) (a) Holter, H.; Møller, K. M. Exptl. Cell. Res. 1956, 15, 631. (b) Laurent, T. C.; Granath, K. A. Biochim. Biophys. Acta 1967, 136, 191.
(14) Haller, W.; Basedow, A. M.; Konig, B. J. Chromatogr. 1977, 132, 387.
(15) Poltevin, E.; Wahl, P. Biophys. Chem. 1988, 31, 247.
(16) Kato, T.; Katsuki, T.; Takahashi, A. Macromolecules 1984, 17, 1726.
(17) Kawahara, K.; Ohta, K.; Miyamoto, H.; Nakamura, S. Carbohydr. Polym. 1984, 4, 335.
(18) Dubin, P. L.; Principi, J. M. J. Chromatogr. 1989, 479, 159.
(19) Amu, T. C. Biophys. Chem. 1982, 16, 269.
(20) A typographical error in ref 15 gives the exponent in eq 8 without the negative sign.
(21) Abramowitz, M.; Stegun, I. Handbook of Mathematical Functions; NBS Applied Mathematics Series; NBS: Washington, D.C., 1990; Vol. 55.
(22) Dubin, P. L.; Kaplan, J. L.; Tian, B.-S.; Mehta, M. J. Chromatogr. 1990, 515, 37.
(23) Granath, K. Private communication.
(24) Lavrenko, P. N.; Mikryukova, O. I.; Didenko, S. A. Polym. Sci. U.S.S.R. 1986, 28, 576 (translation of Vysokomol. Soed. 1986, A28, 517.)
(25) Davidson, M. G.; Deen, W. M. Macromolecules 1988, 21, 3474. (b) Bohrer, M. P.; Patterson, G. D.; Carroll, P. J. Macromolecules 1984, 17, 1170.
(26) Luby-Phelps, K.; Castle, P. E.; Taylor, D. L.; Lanni, F. Proc. Natl. Acad. Sci. U.S.A. 1987, 84, 4910.
(27) Dubin, P. L.; Wright, K. L.; Koontz, S. W. J. Polym. Sci., Polym. Chem. Ed. 1977, 15, 2047.
(28) Phillies, G. D. J. Anal. Chem. 1990, 62, 1049A and references therein.
(29) When the data reported in ref 22 and 23 are superimposed, different dependences of $[\eta]$ on M are not seen; the different values of a reported arise from the sensitivity of a to decisions involved in establishing the best-fit line.
(30) Hagel, L. in Aqueous Size Exclusion Chromatography; Dubin, P. L., Ed.; Elsevier: Amsterdam, 1988; Chapter 5.
(31) Frigon, R. P.; Leypoldt, J. K.; Uyeji, S.; Henderson, L. W. Anal. Chem. 1983, 55, 1349.
(32) Dubin, P. L.; Principi, J. M. Macromolecules 1989, 22, 1891.
(33) Dubin, P. L.; Principi, J. M.; Smith, B. A.; Fallon, M. A. J. Colloid Interface Sci. 1989, 127, 558.

RECEIVED for review December 3, 1990. Accepted February 26, 1991. This work was supported by the donors of the Petroleum Research Fund administered by the American Chemical Society, and Grant CHE-9021484 from the National Science Foundation.

Simultaneous Determination of Inorganic Arsenic and Antimony Species in Natural Waters Using Selective Hydride Generation with Gas Chromatography/Photoionization Detection

Lynda S. Cutter, Gregory A. Cutter,* and Maria L. C. San Diego-McGlone

Department of Oceanography, Old Dominion University, Norfolk, Virginia 23529-0276

Dissolved arsenic and antimony in natural waters can exist in the trivalent and pentavalent oxidation states, and the biochemical and geochemical reactivities of these elements are dependent upon their chemical forms. A method for the simultaneous determination of As(III) + Sb(III) and As(III + V) + Sb(III + V) has been developed that uses selective hydride generation, liquid nitrogen cooled trapping, and gas chromatography/photoionization detection. The detection limit for arsenic is 10 pmol/L, while that for antimony is 3.3 pmol/L; precision (as relative standard deviation) for both elements is better than 3%. The apparatus is rugged and allows determinations to be made in the field. In addition to determining dissolved arsenic and antimony species, an oxidative digest has been developed to allow the simultaneous determination of the two elements in sediments and biogenic particles. Numerous water and particulate samples have been analyzed by using the described procedures.

INTRODUCTION

In natural waters the metalloid elements (e.g., As, Sb, Se) can exist in a variety of oxidation states and chemical forms within a given oxidation state (*1-3*). Thus, the determination of the chemical forms of metalloid elements is an essential part of studying their biogeochemical cycles. Furthermore, the chemical forms of selenium and arsenic have been used to estimate the redox intensity in rainwater (e.g., refs 4, 5). The conventional method for speciating metalloids involves selective hydride generation and atomic absorption detection. While this method has sufficiently low detection limits for concentrations found in natural waters (i.e., nano- to picomolar), each element must be determined individually. The simultaneous determination of metalloid species therefore presents a significant advantage.

Recently, Vien and Fry (*6*) reported a method for the simultaneous determination of total arsenic, antimony, selenium, and tin using hydride generation, gas chromatographic separation of the volatile hydrides, and detection by photoionization. Unfortunately, the chemical conditions required to selectively generate hydrides from the different forms of these elements are mutually exclusive (i.e., iodide must be present to quantitatively generate stibine (SbH_3) from Sb(V), but iodide interferes in the determination of selenium). However, the chemical conditions for selectively generating hydrides from arsenic and antimony species are sufficiently similar to allow their simultaneous determinations. This paper describes a method that is specifically designed to determine these elements in natural waters, with the required detection limits and analytical precision. Further, the apparatus is rugged and can be used for shipboard determinations. Since the chemical forms of arsenic and antimony are not stable during conventional sample storage (e.g., acidification), de-

0003-2700/91/0363-1138$02.50/0